

# Enhancing Polymer Performance Through Graphene Sheets

Jingjing Qiu,<sup>1</sup> Shiren Wang<sup>2</sup>

<sup>1</sup>Department of Mechanical Engineering, Texas Tech University, Lubbock, Texas 79409

<sup>2</sup>Department of Industrial Engineering, Texas Tech University, Lubbock, Texas 79409

Received 9 May 2010; accepted 15 July 2010

DOI 10.1002/app.33068

Published online 30 September 2010 in Wiley Online Library (wileyonlinelibrary.com).

**ABSTRACT:** Graphene sheets were synthesized through intercalation and subsequent ultrasonic processing of graphite natural flakes. The resultant graphene has been characterized by X-ray diffraction, atomic force microscope and transmission electron microscope, and it was confirmed to be exfoliated into monolayer state. The exfoliated graphene was incorporated into epoxy resins and their mechanical performance was investigated. The critical stress fracture intensity factor,  $K_{Ic}$ , was calculated based on the three-point bending test, indicating that the toughness was increased by 41% with addition of

0.54 vol % exfoliated graphene in comparison with the neat resin. The tensile tests also suggested that the elastic modulus and tensile strength were increased by 25 and 10%, respectively. The fracture surface of modified epoxy resins was also examined by scanning electron microscope, and it showed typical features of ductile materials. This study provides a cost-effective way to reinforce polymers for engineering applications. © 2010 Wiley Periodicals, Inc. *J Appl Polym Sci* 119: 3670–3674, 2011

**Key words:** composites; nanoparticle; nanotechnology

## INTRODUCTION

Polymer composites have demonstrated exceptional specific modulus, specific strength and showed widely applications in aerospace, automobile, and deep-water exploration. Filling nanoparticles into polymer matrix is expected to significantly improve their mechanical performance and enable other functionalities. Many efforts have been made to incorporate nanoclays and carbon nanotubes into polymer nanocomposites, and significant progress has been made.<sup>1–6</sup> Graphene, a monolayer of carbon atoms arranged in a honeycomb network or an un-rolled single-walled carbon nanotube, recently have attracted significant attentions.<sup>7–9</sup> Much like carbon nanotubes, it demonstrates excellent electric conductivity and thermal conductivity. Its mechanical properties are also comparable to carbon nanotubes, demonstrating outstanding stiffness and flexibility. Hone's research group at Columbia University has recently measured the mechanical properties of single graphene by nanoindentation, indicating that Young's modulus is  $\sim 1$  TPa, and strength 130 GPa.<sup>10</sup> Recent studies suggested that the production cost of graphene in large quantities can be much lower than car-

bon nanotubes. Currently, graphene sheets can be achieved by graphite exfoliation, including mechanical cleavage of graphite,<sup>11–13</sup> chemical exfoliation of graphite,<sup>14–18</sup> and direct synthesis, such as epitaxial growth,<sup>19,20</sup> Bottom-up synthesis.<sup>21</sup> With respect to large scale production of graphene, chemical exfoliation methods receive the most attention and are used widely. Incorporation of graphene into polymers is expected to significantly enhance their mechanical properties at low volume fractions. Due to the nature of two-dimensional nanostructure, graphene is also anticipated to improve barrier properties and other functionality of polymer composites at low volume fractions.

As one of the most popular matrixes in the polymer composite, epoxy resins have demonstrated outstanding stiffness, specific strength, dimensional stability, and chemical resistance, and shown considerable adhesion to the embedded fiber. In addition to composite matrix, they have been extensively used in various fields of coating, high-performance adhesives, etc. In this article, chemically exfoliated graphene is used to enhance epoxy resins. The mechanical properties of resulted nanocomposites were measured by three-point bending and tensile tests. Scanning electron microscopy (SEM) was used to characterize the fracture surface.

## EXPERIMENTAL

Graphite (Nature flake graphite, sized at 45  $\mu\text{m}$  (Grade 230), was kindly provided by Asbury

Correspondence to: S. Wang (shiren.wang@ttu.edu).

Contract grant sponsor: Texas Tech University.

Contract grant sponsor: National Science Foundation; contract grant number: CMMI#0953674.

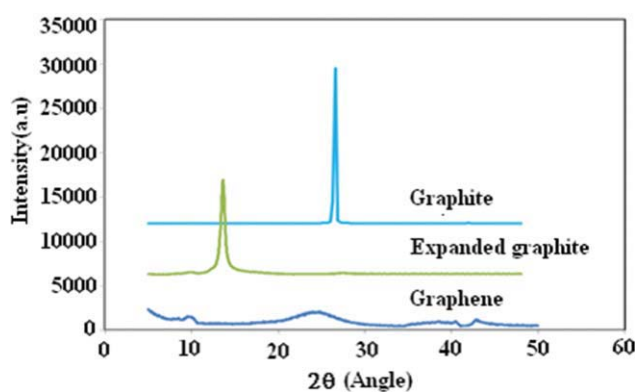


**Figure 1** WXR D of graphite, expanded graphite, and graphene materials. [Color figure can be viewed in the online issue, which is available at [wileyonlinelibrary.com](http://wileyonlinelibrary.com).]

Carbons (Asbury, NJ). Sodium chlorate, nitric acid, and hydrochloric acid were purchased from Fisher Scientific Inc. Epoxy resin (Brand: Epon862) was provided by Hexion Inc at Houston, Texas. Graphite was expanded and oxidized according to the modified Brodie's method.<sup>22</sup> Ten gram graphite, 160 mL nitric acid, and 85 g sodium chlorate were mixed at room temperature. The mixture was kept for 24 h under stirring. Then it was washed with  $5 \times 200$  mL 5% hydrochloric acid and  $7 \times 1$  L distilled water. When the acidic and saline impurities were removed, the expanded graphite oxide was achieved through sedimentation and finally dried at 60°C. The resultant expanded graphite oxidize was further exfoliated under the ultrasonic processing in the poly (styrenesulfonate)-dispersed aqueous solutions, resulting in individualized graphene oxide (GO) sheet. The suspension was further subjected to ultracentrifugation and top solutions were collected, resulting in exfoliated graphene films.

This exfoliated GO membrane was broken into pieces and ground to paste in a small amount of acetone. A certain curing agent (based on the required curing ratio) was weighed and added to the GO paste. Subsequently, GO and curing agent were mixed in the acetone solvent under cup-horn ultrasonic processing at 30 W for half an hour. The mixture of GO and curing agent were then transferred to the diluted epoxy resin, resulting in a new mixture which was processed with cup-horn ultrasonic processing at the power of 12 W for 3 h. Finally, the mixture was shearing for 10 h by digital lab mixer under 1000 rpm. The resultant mixture of GO and epoxy resin was left in the vacuum system for 12 h to remove the residual solvent. The final mixture was cast into a metallic mold and cured under hot-press at 177°C for 2.5 h. The subsequent post-cure was conducted at 177°C for another 2 h. The graphite-filled epoxy resin was prepared in the same procedure. The

loading of GO and graphite-filled epoxy resin was both at 0.54% by volume.

The graphite and graphene were characterized with wide-angle X-ray diffraction (WXR D). The tensile test of enhanced polymer was performed by Shimadzu AGS-J machine. The fracture toughness of nanocomposites was tested by MTS instrument (MTS 858, MTS Systems Corporation) according to the ASTM E1820. Fracture surface was characterized with JEOL SEM.

## RESULTS AND DISCUSSIONS

The pristine graphite (PG), expanded graphite and exfoliated GO were characterized by WXR D and their spectra are shown in Figure 1. For the PG sample, the (002) peak appears at 27°, indicating an interlayer-spacing of 0.34 nm. After oxidation-induced expansion, the (002) peak shifts to 12°, suggesting that the interlayer distance increased to 0.72 nm. These results are consistent with the data reported in the literatures.<sup>16,17,23</sup> After ultrasonic processing and subsequent ultracentrifugation, the resulting exfoliated GO did not show any sharp peak as expanded graphite and PG do, but show a very weak and broad peak near 25°. This may stem from the change of lattice structure. Exfoliated graphene was in the state of monolayer or few layers and this kind of lattice structure is significantly different from PG crystal.

The aqueous solution of exfoliated graphene sheets was dropped onto silicon substrate and characterized by atomic force microscope (AFM). The thickness of suspended graphene sheets was measured by section analysis as shown in Figure 2. The measurement indicates their thickness is 0.8 ~ 1.6 nm, suggesting that graphene in a mono-layer or few-layer state was achieved. This result agrees with the literature report regarding exfoliated graphene.<sup>7,16,17,23</sup> Generally, single-layer graphene is always ~ 1 nm thick in AFM images due to the following reasons: attached molecules on the graphene surface, imperfect interface between graphene and silicon substrate, and possible

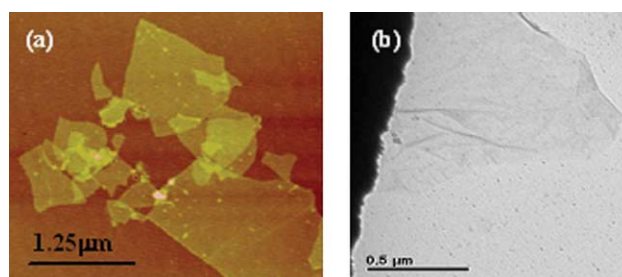


**Figure 2** (a) AFM image of graphene and (b) TEM image of graphene. [Color figure can be viewed in the online issue, which is available at [wileyonlinelibrary.com](http://wileyonlinelibrary.com).]

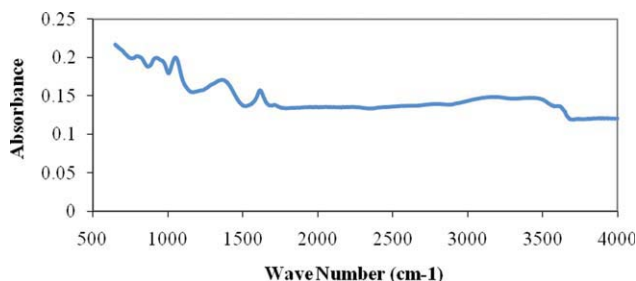


**Figure 3** FT-IR of graphene oxide sheets. [Color figure can be viewed in the online issue, which is available at [wileyonlinelibrary.com](http://wileyonlinelibrary.com).]

different attraction force between AFM probes, when compared with silicon substrate.<sup>7</sup> Transmission electron microscope (TEM) was also used to characterize the exfoliated graphene sheets and the image is shown in Figure 2(b), confirming the exfoliation state of graphene sheets. It is interesting to find that there are many wrinkles on the graphene sheet and it is not ideally flat.

The GO sheets were also characterized by FT-IR, as shown in Figure 3. The C—OH stretching peak is observed at  $\sim 3600/\text{cm}$ . The absorption peaks at 801.6, 928.1, and 1054.7/ $\text{cm}$  are contributed from epoxy group.<sup>24–26</sup> The vibration peak at 1360/ $\text{cm}$  is contributed from C—OH bending.<sup>15,16</sup> The sharp peak at 1615.3/ $\text{cm}$  should be credited to the water absorption. These vibration peaks verified the successful attachment of epoxide and hydroxyl.

In addition, the weight percentage of epoxide and hydroxyl was estimated by TGA. GO was tested by TGA in the air environment and results are shown in Figure 4. The weight loss in the beginning should be caused by evaporation of moistures. The onset temperature for GO is 270°C, and the weight loss is around 23%, indicating about 23% of epoxide and hydroxyl groups.

Fracture toughness of neat epoxy resins and graphene-filled nanocomposites was determined from static three-point bending tests of single edge notch

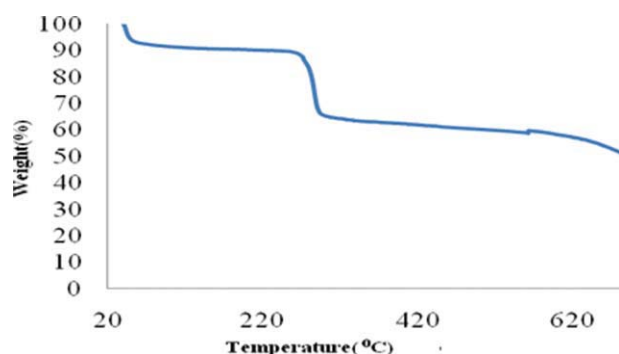


**Figure 4** TGA results of graphene oxide. [Color figure can be viewed in the online issue, which is available at [wileyonlinelibrary.com](http://wileyonlinelibrary.com).]

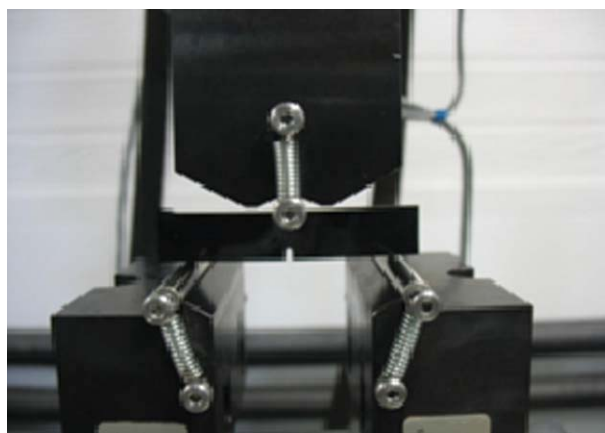


**Figure 5** Three-point bending test on MTS instrument.

specimens according to the ASTM E1820. The testing setup is shown in Figure 5. The span is four times of width.

During the test, the change in specimen length was measured by recording the ram positions through the displacement transducer of the MTS machine. The critical stress intensity factor,  $K_{1c}$ , was calculated according to the following equations:

$$K_{1c} = \left( \frac{PS}{Bw^{3/2}} \right) f(a/w)$$

where  $P$ : applied load on the specimen;  $B$ : specimen thickness;  $w$ : specimen width;  $a$ : crack evolution length.

$f(a/w)$

$$= \frac{3\left(\frac{a}{w}\right)^{1/2} \left[ 1.99 - \left(\frac{a}{w}\right) \left(1 - \frac{a}{w}\right) \right] (2.15 - 3.93\left(\frac{a}{w}\right) + 2.7\left(\frac{a}{w}\right))}{2\left(1 + 2\left(\frac{a}{w}\right)\right) \left(1 - \frac{a}{w}\right)^{3/2}}$$

The  $K_{1c}$  was calculated and indicated that GO significantly improved the toughness of epoxy resin at

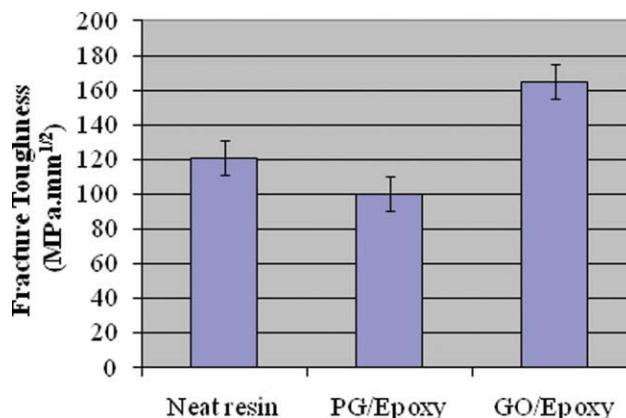


**Figure 6** Toughness of modified epoxy resins. [Color figure can be viewed in the online issue, which is available at [wileyonlinelibrary.com](http://wileyonlinelibrary.com).]



**TABLE I**  
**Tensile Properties of Graphene Nanocomposites**

Sample	Neat resin	PG/epoxy	GO/epoxy
Elastic modulus (GPa)	2.0	2.35	2.49
Tensile strength (MPa)	72.6	45	79.0037

0.54% loading by volume, as shown in Figure 6. The GO modified epoxy shows a toughness  $K_{1C}$  with an increase of  $\sim 41\%$  in comparison with neat resins. However, addition of PG did not demonstrate improvement and this is probably due to the graphite internal sliding and weak interface between PG and resin when load was applied. GO shows hydroxyl and epoxy group on the surface while graphite shows no chemical groups. Poor interfacial bonding will significantly affect the load transfer from polymer matrix to particles. Graphite consists of many layers of graphene and it is very easy to slide when external force is applied. This sliding will also decrease the load transfer between polymer matrix and the particles.

Besides improving the toughness of the epoxy resins, we do not want to reduce any mechanical properties. Hence, the modified epoxy resins were also cured and molded to standard double-bell samples according to ASME D638 standard. The average tensile results were summarized in Table I. Through incorporation of low fraction of GO, the elastic modulus was increased  $\sim 25\%$  and tensile strength was enhanced  $\sim 10\%$  in comparison with neat resins. Traditional rubble-toughening method usually leads to low modulus when the resin toughness is improved.<sup>1-4</sup> Hence, filling graphene shows obvious advantage and potential engineering applications.

The fracture surface of modified epoxy resins was also investigated by scanning electron microscope (SEM), and the results are shown in Figure 7. The neat epoxy resins fracture surface demonstrates typical brittle fracture characteristics and shows "river-like" fracture patterns initialized from the cracks. After the crack initiated, the crack propagated rapidly in the brittle materials. During propa-

gation, more and more cracks merged and expanded, resulting in river-like patterns. The area between the "river-like" patterns is very smooth, indicating the rapid crack propagating. The graphite modified epoxy resin fracture surface also produces similar "river-like" fracture patterns, whereas GO modified epoxy resin shows quite different fracture morphology. The surface appeared coarser and ductile by showing many fracture ditches and obvious plastic deformations. This indicates that the GO increased the toughness of the materials by effectively preventing the crack propagation. The crack moves slowly and is accompanied by a large amount of plastic deformation. The crack will usually not extend unless an increased stress is applied. Therefore, the crack evolutions have to frequently change direction and continue propagating toward the weak area in the modified resin matrix. This consumes more energy and causes the rougher fracture surface. The graphene sheets were also observed to be tightly embedded into polymer matrix, as shown in Figure 7(d).

## CONCLUSION

Graphite was exfoliated through a chemical method and the resultant graphene was applied to enhance epoxy resin. With only 0.54% loading by volume, the resultant nanocomposites were considerably reinforced. The critical stress intensity factor,  $K_{1C}$ , was calculated according to the three-point bending test, and suggested that the toughness was increased by 41%. In addition, both elastic modulus and tensile strength were also improved. SEM characterization of the fracture surface also confirmed the improved fracture toughness. With addition of small percentage of exfoliated graphene, fracture surface appeared coarser and ductile by showing many fracture ditches and obvious plastic deformations. This study provides a cost-effective way to enhance polymers and expands their industrial applications.

The authors thank Asbury Carbons for providing the natural graphite materials.

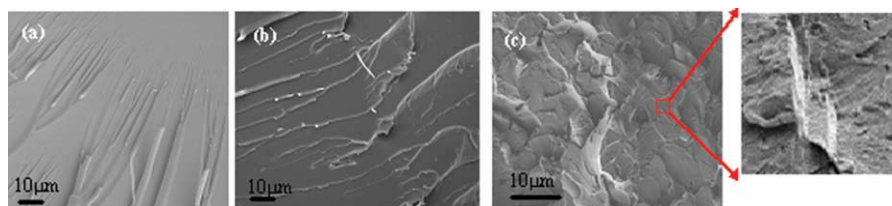


**Figure 7** SEM image of fracture surface. (a) Neat resin; (b) graphite/epoxy; (c) graphene oxide/epoxy system; and (d) graphene embedded into epoxy matrix. [Color figure can be viewed in the online issue, which is available at [www.interscience.wiley.com](http://www.interscience.wiley.com).]

## References

1. Alexandre, M.; Dubois, P. *Mater Sci Eng R Rep* 2000, 28, 1.
2. Moniruzzaman, M.; Winey, K. I. *Macromolecules* 2006, 39, 5194.
3. Wang, S.; Liang, R.; Wang, B.; Zhang, C. *Polym Compos* 2009, 30, 1050.
4. Dean, D.; Walker, R.; Theodore, M.; Hampton, E.; Nyairo, E. *Polymer* 2005, 48, 3014.
5. Wang, S.; Liang, R.; Wang, B.; Zhang, C. *Chem Phys Lett* 2008, 457, 371.
6. Wang, S.; Liang, R.; Wang, B.; Zhang, C. *Nanotechnology* 2008, 19, 085710.
7. Rafiee, M. A.; Refiee, J.; Wang, Z.; Song, H.; Yu, Z.-Z.; Koratkar, N. *ACS Nano* 2009, 3, 3884.
8. Stankovich, S.; Dikin, D. A.; Dommett, G. H. B.; Kohlhaas, K. M.; Zimney, E. J.; Stach, E. A.; Piner, R. D.; Nguyen, S. T.; Ruoff, R. S. *Nature* 2006, 442, 282.
9. Li, D.; Kaner, R. B. *Science* 2008, 320, 1170.
10. Lee, C.; Wei, X.; Kysar, J. W.; Hone, J. *Science* 2008, 321, 385.
11. Novoselov, K. S.; Geim, A. K.; Morozov, S. V.; Jiang, D.; Zhang, Y.; Dubonos, S. V.; Grigorieva, I. V.; Firsov, A. A. *Science* 2004, 306, 666.
12. Novoselov, K. S.; Jiang, D.; Schedin, F.; Booth, T. J.; Khotkevich, V. V.; Morozov, S. V.; Geim, A. K. *Proc Natl Acad Sci* 2005, 102, 10451.
13. Faugeras, C.; Nerriere, A.; Potemski, M.; Mahmood, A.; Dujardin, E.; Berger, C.; de Heer, W. A. *Appl Phys Lett* 2008, 92, 011914.
14. Jeong, H. K.; Lee, Y. P.; Lahaye, R. J.; Park, M. H.; An, K. H.; Kim, I. J.; Yang, C. -W.; Park, C. Y.; Ruoff, R. S.; Lee, Y. H. *J Am Chem Soc* 2008, 130, 1362.
15. Stankovich, S.; Piner, R. D.; Nguyen, S. B. T.; Ruoff, R. S. *Carbon* 2006, 44, 3342.
16. Xu, C.; Xu, X.; Zhu, J.; Wang, X. *Carbon* 2008, 46, 365.
17. Szabo, T.; Berkesi, O.; Forgo, P.; Josepovits, K.; Sanakis, Y.; Petridis, D.; Dekany, I. *Chem Mater* 2006, 18, 2740.
18. Eda, G.; Fanchini, G.; Chhowalla, M. *Nature Nanotechnol* 2008, 3, 270.
19. Geim, A. K.; Novoselov, K. S. *Nature Mater* 2007, 6, 183.
20. Berger, C.; Song, Z.; Li, X.; Wu, X.; Brown, N.; Naud, C.; Mayou, D.; Li, T.; Hass, J.; Marchenkov, A. N.; Conrad, E. H.; First, P. N.; de Heer, W. A. *Science* 2006, 312, 1191.
21. Wu, J. S.; Pisula, W.; Mullen, K. *Chem Rev* 2007, 107, 718.
22. Wang, S.; Tambraparni, M.; Qiu, J.; Tipton, J.; Dean, D. *Macromolecules* 2009, 42, 5251.
23. Herrera-Alonso, M.; Abdada, A. A.; McAllister, M. J.; Aksay, I. A.; Prud'homme, R. K. *Langmuir* 2007, 23, 10644.
24. Mao, Y.; Gleason, K. K. *Langmuir* 2004, 20, 2484.
25. Vandijkwolthuis, W. N.; Franssen, O.; Talsma, H.; Vansteenberghe, M. J.; Vandenbosch, J. J.; Hennink, W. E. *Macromolecules* 1995, 28, 6317.
26. Wang, S.; Liang, R.; Wang, B.; Zhang, C. *Carbon* 2007, 45, 3047.